PHYSICAL REVIEW D **77,** 071102(R) (2008)

Time-dependent Dalitz plot analysis of $B^0 \to D^{\mp} K^0 \pi^{\pm}$ decays

B. Aubert,[1] M. Bona,[1] Y. Karyotakis,[1] J. P. Lees,[1] V. Poireau,[1] X. Prudent,[1] V. Tisserand,[1] A. Zghiche,[1] J. Garra Tico,[2] E. Grauges,[2] L. Lopez,[3] A. Palano,[3] M. Pappagallo,[3] G. Eigen,[4] B. Stugu,[4] L. Sun,[4] G. S. Abrams,[5] M. Battaglia,[5] D. N. Brown,[5] J. Button-Shafer,[5] R. N. Cahn,[5] R. G. Jacobsen,[5] J. A. Kadyk,[5] L. T. Kerth,[5] Yu. G. Kolomensky,[5] G. Kukartsev,[5] D. Lopes Pegna,[5] G. Lynch,[5] T. J. Orimoto,[5] I. L. Osipenkov,[5] M. T. Ronan,[5,*] K. Tackmann,[5] T. Tanabe,[5] W. A. Wenzel,[5] P. del Amo Sanchez,[6] C. M. Hawkes,[6] N. Soni,[6] A. T. Watson,[6] H. Koch,[7] T. Schroeder,[7] D. Walker,[8] D. J. Asgeirsson,[9] T. Cuhadar-Donszelmann,[9] B. G. Fulsom,[9] C. Hearty,[9] T. S. Mattison,[9] J. A. McKenna,[9] M. Barrett,[10] A. Khan,[10] M. Saleem,[10] L. Teodorescu,[10] V. E. Blinov,[11] A. D. Bukin,[11] A. R. Buzykaev,[11] V. P. Druzhinin,[11] V. B. Golubev,[11] A. P. Onuchin,[11] S. I. Serednyakov,[11] Yu. I. Skovpen,[11] E. P. Solodov,[11] K. Yu. Todyshev,[11] M. Bondioli,[12] S. Curry,[12] I. Eschrich,[12] D. Kirkby,[12] A. J. Lankford,[12] P. Lund,[12] M. Mandelkern,[12] E. C. Martin,[12] D. P. Stoker,[12] S. Abachi,[13] C. Buchanan,[13] J. W. Gary,[14] F. Liu,[14] O. Long,[14] B. C. Shen,[14,*] G. M. Vitug,[14] L. Zhang,[14] H. P. Paar,[15] S. Rahatlou,[15] V. Sharma,[15] J. W. Berryhill,[16] C. Campagnari,[16] A. Cunha,[16] B. Dahmes,[16] T. M. Hong,[16] D. Kovalskyi,[16] J. D. Richman,[16] T. W. Beck,[17] A. M. Eisner,[17] C. J. Flacco,[17] C. A. Heusch,[17] J. Kroseberg,[17] W. S. Lockman,[17] T. Schalk,[17] B. A. Schumm,[17] A. Seiden,[17] M. G. Wilson,[17] L. O. Winstrom,[17] E. Chen,[18] C. H. Cheng,[18] B. Echenard,[18] F. Fang,[18] D. G. Hitlin,[18] I. Narsky,[18] T. Piatenko,[18] F. C. Porter,[18] R. Andreassen,[19] G. Mancinelli,[19] B. T. Meadows,[19] K. Mishra,[19] M. D. Sokoloff,[19] F. Blanc,[20] P. C. Bloom,[20] W. T. Ford,[20] J. F. Hirschauer,[20] A. Kreisel,[20] M. Nagel,[20] U. Nauenberg,[20] A. Olivas,[20] J. G. Smith,[20] K. A. Ulmer,[20] S. R. Wagner,[20] J. Zhang,[20] R. Ayad,[21,†] A. M. Gabareen,[21] A. Soffer,[21,‡] W. H. Toki,[21] R. J. Wilson,[21] D. D. Altenburg,[22] E. Feltresi,[22] A. Hauke,[22] H. Jasper,[22] J. Merkel,[22] A. Petzold,[22] B. Spaan,[22] K. Wacker,[22] V. Klose,[23] M. J. Kobel,[23] H. M. Lacker,[23] W. F. Mader,[23] R. Nogowski,[23] J. Schubert,[23] K. R. Schubert,[23] R. Schwierz,[23] J. E. Sundermann,[23] A. Volk,[23] D. Bernard,[24] G. R. Bonneaud,[24] E. Latour,[24] V. Lombardo,[24] Ch. Thiebaux,[24] M. Verderi,[24] P. J. Clark,[25] W. Gradl,[25] F. Muheim,[25] S. Playfer,[25] A. I. Robertson,[25] J. E. Watson,[25] Y. Xie,[25] M. Andreotti,[26] D. Bettoni,[26] C. Bozzi,[26] R. Calabrese,[26] A. Cecchi,[26] G. Cibinetto,[26] P. Franchini,[26] E. Luppi,[26] M. Negrini,[26] A. Petrella,[26] L. Piemontese,[26] E. Prencipe,[26] V. Santoro,[26] F. Anulli,[27] R. Baldini-Ferroli,[27] A. Calcaterra,[27] R. de Sangro,[27] G. Finocchiaro,[27] S. Pacetti,[27] P. Patteri,[27] I. M. Peruzzi,[27,§] M. Piccolo,[27] M. Rama,[27] A. Zallo,[27] A. Buzzo,[28] R. Contri,[28] M. Lo Vetere,[28] M. M. Macri,[28] M. R. Monge,[28] S. Passaggio,[28] C. Patrignani,[28] E. Robutti,[28] A. Santroni,[28] S. Tosi,[28] K. S. Chaisanguanthum,[29] M. Morii,[29] J. Wu,[29] R. S. Dubitzky,[30] J. Marks,[30] S. Schenk,[30] U. Uwer,[30] D. J. Bard,[31] P. D. Dauncey,[31] J. A. Nash,[31] W. Panduro Vazquez,[31] M. Tibbetts,[31] P. K. Behera,[32] X. Chai,[32] M. J. Charles,[32] U. Mallik,[32] J. Cochran,[33] H. B. Crawley,[33] L. Dong,[33] V. Eyges,[33] W. T. Meyer,[33] S. Prell,[33] E. I. Rosenberg,[33] A. E. Rubin,[33] Y. Y. Gao,[34] A. V. Gritsan,[34] Z. J. Guo,[34] C. K. Lae,[34] A. G. Denig,[35] M. Fritsch,[35] G. Schott,[35] N. Arnaud,[36] J. Béquilleux,[36] A. D'Orazio,[36] M. Davier,[36] G. Grosdidier,[36] A. Höcker,[36] V. Lepeltier,[36] F. Le Diberder,[36] A. M. Lutz,[36] S. Pruvot,[36] P. Roudeau,[36] M. H. Schune,[36] J. Serrano,[36] V. Sordini,[36] A. Stocchi,[36] W. F. Wang,[36] G. Wormser,[36] D. J. Lange,[37] D. M. Wright,[37] I. Bingham,[38] J. P. Burke,[38] C. A. Chavez,[38] J. R. Fry,[38] E. Gabathuler,[38] R. Gamet,[38] D. E. Hutchcroft,[38] D. J. Payne,[38] K. C. Schofield,[38] C. Touramanis,[38] A. J. Bevan,[39] K. A. George,[39] F. Di Lodovico,[39] R. Sacco,[39] G. Cowan,[40] H. U. Flaecher,[40] D. A. Hopkins,[40] S. Paramesvaran,[40] F. Salvatore,[40] A. C. Wren,[40] D. N. Brown,[41] C. L. Davis,[41] N. R. Barlow,[42] R. J. Barlow,[42] Y. M. Chia,[42] C. L. Edgar,[42] G. D. Lafferty,[42] T. J. West,[42] J. I. Yi,[42] J. Anderson,[43] C. Chen,[43] A. Jawahery,[43] D. A. Roberts,[43] G. Simi,[43] J. M. Tuggle,[43] C. Dallapiccola,[44] S. S. Hertzbach,[44] X. Li,[44] T. B. Moore,[44] E. Salvati,[44] S. Saremi,[44] R. Cowan,[45] D. Dujmic,[45] P. H. Fisher,[45] K. Koeneke,[45] G. Sciolla,[45] M. Spitznagel,[45] F. Taylor,[45] R. K. Yamamoto,[45] M. Zhao,[45] S. E. Mclachlin,[46,*] P. M. Patel,[46] S. H. Robertson,[46] A. Lazzaro,[47] F. Palombo,[47] J. M. Bauer,[48] L. Cremaldi,[48] V. Eschenburg,[48] R. Godang,[48] R. Kroeger,[48] D. A. Sanders,[48] D. J. Summers,[48] H. W. Zhao,[48] S. Brunet,[49] D. Côté,[49] M. Simard,[49] P. Taras,[49] F. B. Viaud,[49] H. Nicholson,[50] G. De Nardo,[51] F. Fabozzi,[51,‖] L. Lista,[51] D. Monorchio,[51] C. Sciacca,[51] M. A. Baak,[52] G. Raven,[52] H. L. Snoek,[52] C. P. Jessop,[53] K. J. Knoepfel,[53] J. M. LoSecco,[53] G. Benelli,[54] L. A. Corwin,[54] K. Honscheid,[54] H. Kagan,[54] R. Kass,[54] J. P. Morris,[54] A. M. Rahimi,[54] J. J. Regensburger,[54] S. J. Sekula,[54] Q. K. Wong,[54] N. L. Blount,[55] J. Brau,[55] R. Frey,[55] O. Igonkina,[55] J. A. Kolb,[55] M. Lu,[55] R. Rahmat,[55] N. B. Sinev,[55] D. Strom,[55] J. Strube,[55] E. Torrence,[55] N. Gagliardi,[56] A. Gaz,[56] M. Margoni,[56] M. Morandin,[56] A. Pompili,[56] M. Posocco,[56] M. Rotondo,[56] F. Simonetto,[56] R. Stroili,[56] C. Voci,[56] E. Ben-Haim,[57] H. Briand,[57] G. Calderini,[57] J. Chauveau,[57] P. David,[57] L. Del Buono,[57] Ch. de la Vaissière,[57] O. Hamon,[57] Ph. Leruste,[57] J. Malclès,[57] J. Ocariz,[57] A. Perez,[57] J. Prendki,[57] L. Gladney,[58] M. Biasini,[59] R. Covarelli,[59] E. Manoni,[59] C. Angelini,[60] G. Batignani,[60] S. Bettarini,[60] M. Carpinelli,[60,¶] R. Cenci,[60] A. Cervelli,[60] F. Forti,[60] M. A. Giorgi,[60] A. Lusiani,[60] G. Marchiori,[60] M. A. Mazur,[60] M. Morganti,[60] N. Neri,[60] E. Paoloni,[60] G. Rizzo,[60]

J. J. Walsh,[60] J. Biesiada,[61] Y. P. Lau,[61] C. Lu,[61] J. Olsen,[61] A. J. S. Smith,[61] A. V. Telnov,[61] E. Baracchini,[62] F. Bellini,[62] G. Cavoto,[62] D. del Re,[62] E. Di Marco,[62] R. Faccini,[62] F. Ferrarotto,[62] F. Ferroni,[62] M. Gaspero,[62] P. D. Jackson,[62] M. A. Mazzoni,[62] S. Morganti,[62] G. Piredda,[62] F. Polci,[62] F. Renga,[62] C. Voena,[62] M. Ebert,[63] T. Hartmann,[63] H. Schröder,[63] R. Waldi,[63] T. Adye,[64] G. Castelli,[64] B. Franek,[64] E. O. Olaiya,[64] W. Roethel,[64] F. F. Wilson,[64] S. Emery,[65] M. Escalier,[65] A. Gaidot,[65] S. F. Ganzhur,[65] G. Hamel de Monchenault,[65] W. Kozanecki,[65] G. Vasseur,[65] Ch. Yèche,[65] M. Zito,[65] X. R. Chen,[66] H. Liu,[66] W. Park,[66] M. V. Purohit,[66] R. M. White,[66] J. R. Wilson,[66] M. T. Allen,[67] D. Aston,[67] R. Bartoldus,[67] P. Bechtle,[67] R. Claus,[67] J. P. Coleman,[67] M. R. Convery,[67] J. C. Dingfelder,[67] J. Dorfan,[67] G. P. Dubois-Felsmann,[67] W. Dunwoodie,[67] R. C. Field,[67] T. Glanzman,[67] S. J. Gowdy,[67] M. T. Graham,[67] P. Grenier,[67] C. Hast,[67] W. R. Innes,[67] J. Kaminski,[67] M. H. Kelsey,[67] H. Kim,[67] P. Kim,[67] M. L. Kocian,[67] D. W. G. S. Leith,[67] S. Li,[67] S. Luitz,[67] V. Luth,[67] H. L. Lynch,[67] D. B. MacFarlane,[67] H. Marsiske,[67] R. Messner,[67] D. R. Muller,[67] S. Nelson,[67] C. P. O'Grady,[67] I. Ofte,[67] A. Perazzo,[67] M. Perl,[67] T. Pulliam,[67] B. N. Ratcliff,[67] A. Roodman,[67] A. A. Salnikov,[67] R. H. Schindler,[67] J. Schwiening,[67] A. Snyder,[67] D. Su,[67] M. K. Sullivan,[67] K. Suzuki,[67] S. K. Swain,[67] J. M. Thompson,[67] J. Va'vra,[67] A. P. Wagner,[67] M. Weaver,[67] W. J. Wisniewski,[67] M. Wittgen,[67] D. H. Wright,[67] H. W. Wulsin,[67] A. K. Yarritu,[67] K. Yi,[67] C. C. Young,[67] V. Ziegler,[67] P. R. Burchat,[68] A. J. Edwards,[68] S. A. Majewski,[68] T. S. Miyashita,[68] B. A. Petersen,[68] L. Wilden,[68] S. Ahmed,[69] M. S. Alam,[69] R. Bula,[69] J. A. Ernst,[69] B. Pan,[69] M. A. Saeed,[69] S. B. Zain,[69] S. M. Spanier,[70] B. J. Wogsland,[70] R. Eckmann,[71] J. L. Ritchie,[71] A. M. Ruland,[71] C. J. Schilling,[71] R. F. Schwitters,[71] J. M. Izen,[72] X. C. Lou,[72] S. Ye,[72] F. Bianchi,[73] F. Gallo,[73] D. Gamba,[73] M. Pelliccioni,[73] M. Bomben,[74] L. Bosisio,[74] C. Cartaro,[74] F. Cossutti,[74] G. Della Ricca,[74] L. Lanceri,[74] L. Vitale,[74] V. Azzolini,[75] N. Lopez-March,[75] F. Martinez-Vidal,[75] D. A. Milanes,[75] A. Oyanguren,[75] J. Albert,[76] Sw. Banerjee,[76] B. Bhuyan,[76] K. Hamano,[76] R. Kowalewski,[76] I. M. Nugent,[76] J. M. Roney,[76] R. J. Sobie,[76] P. F. Harrison,[77] J. Ilic,[77] T. E. Latham,[77] G. B. Mohanty,[77] H. R. Band,[78] X. Chen,[78] S. Dasu,[78] K. T. Flood,[78] J. J. Hollar,[78] P. E. Kutter,[78] Y. Pan,[78] M. Pierini,[78] R. Prepost,[78] S. L. Wu,[78] and H. Neal[79]

(*BABAR* Collaboration)

[1]*Laboratoire de Physique des Particules, IN2P3/CNRS et Université de Savoie, F-74941 Annecy-Le-Vieux, France*
[2]*Universitat de Barcelona, Facultat de Fisica, Departament ECM, E-08028 Barcelona, Spain*
[3]*Università di Bari, Dipartimento di Fisica and INFN, I-70126 Bari, Italy*
[4]*University of Bergen, Institute of Physics, N-5007 Bergen, Norway*
[5]*Lawrence Berkeley National Laboratory and University of California, Berkeley, California 94720, USA*
[6]*University of Birmingham, Birmingham, B15 2TT, United Kingdom*
[7]*Ruhr Universität Bochum, Institut für Experimentalphysik 1, D-44780 Bochum, Germany*
[8]*University of Bristol, Bristol BS8 1TL, United Kingdom*
[9]*University of British Columbia, Vancouver, British Columbia, Canada V6T 1Z1*
[10]*Brunel University, Uxbridge, Middlesex UB8 3PH, United Kingdom*
[11]*Budker Institute of Nuclear Physics, Novosibirsk 630090, Russia*
[12]*University of California at Irvine, Irvine, California 92697, USA*
[13]*University of California at Los Angeles, Los Angeles, California 90024, USA*
[14]*University of California at Riverside, Riverside, California 92521, USA*
[15]*University of California at San Diego, La Jolla, California 92093, USA*
[16]*University of California at Santa Barbara, Santa Barbara, California 93106, USA*
[17]*University of California at Santa Cruz, Institute for Particle Physics, Santa Cruz, California 95064, USA*
[18]*California Institute of Technology, Pasadena, California 91125, USA*
[19]*University of Cincinnati, Cincinnati, Ohio 45221, USA*
[20]*University of Colorado, Boulder, Colorado 80309, USA*
[21]*Colorado State University, Fort Collins, Colorado 80523, USA*
[22]*Universität Dortmund, Institut für Physik, D-44221 Dortmund, Germany*
[23]*Technische Universität Dresden, Institut für Kern- und Teilchenphysik, D-01062 Dresden, Germany*
[24]*Laboratoire Leprince-Ringuet, CNRS/IN2P3, Ecole Polytechnique, F-91128 Palaiseau, France*
[25]*University of Edinburgh, Edinburgh EH9 3JZ, United Kingdom*
[26]*Università di Ferrara, Dipartimento di Fisica and INFN, I-44100 Ferrara, Italy*
[27]*Laboratori Nazionali di Frascati dell'INFN, I-00044 Frascati, Italy*
[28]*Università di Genova, Dipartimento di Fisica and INFN, I-16146 Genova, Italy*
[29]*Harvard University, Cambridge, Massachusetts 02138, USA*
[30]*Universität Heidelberg, Physikalisches Institut, Philosophenweg 12, D-69120 Heidelberg, Germany*
[31]*Imperial College London, London, SW7 2AZ, United Kingdom*

[32]University of Iowa, Iowa City, Iowa 52242, USA
[33]Iowa State University, Ames, Iowa 50011-3160, USA
[34]Johns Hopkins University, Baltimore, Maryland 21218, USA
[35]Universität Karlsruhe, Institut für Experimentelle Kernphysik, D-76021 Karlsruhe, Germany
[36]Laboratoire de l'Accélérateur Linéaire, IN2P3/CNRS et Université Paris-Sud 11, Centre Scientifique d'Orsay, B. P. 34, F-91898 ORSAY Cedex, France
[37]Lawrence Livermore National Laboratory, Livermore, California 94550, USA
[38]University of Liverpool, Liverpool L69 7ZE, United Kingdom
[39]Queen Mary, University of London, E1 4NS, United Kingdom
[40]University of London, Royal Holloway and Bedford New College, Egham, Surrey TW20 0EX, United Kingdom
[41]University of Louisville, Louisville, Kentucky 40292, USA
[42]University of Manchester, Manchester M13 9PL, United Kingdom
[43]University of Maryland, College Park, Maryland 20742, USA
[44]University of Massachusetts, Amherst, Massachusetts 01003, USA
[45]Massachusetts Institute of Technology, Laboratory for Nuclear Science, Cambridge, Massachusetts 02139, USA
[46]McGill University, Montréal, Québec, Canada H3A 2T8
[47]Università di Milano, Dipartimento di Fisica and INFN, I-20133 Milano, Italy
[48]University of Mississippi, University, Mississippi 38677, USA
[49]Université de Montréal, Physique des Particules, Montréal, Québec, Canada H3C 3J7
[50]Mount Holyoke College, South Hadley, Massachusetts 01075, USA
[51]Università di Napoli Federico II, Dipartimento di Scienze Fisiche and INFN, I-80126, Napoli, Italy
[52]NIKHEF, National Institute for Nuclear Physics and High Energy Physics, NL-1009 DB Amsterdam, The Netherlands
[53]University of Notre Dame, Notre Dame, Indiana 46556, USA
[54]Ohio State University, Columbus, Ohio 43210, USA
[55]University of Oregon, Eugene, Oregon 97403, USA
[56]Università di Padova, Dipartimento di Fisica and INFN, I-35131 Padova, Italy
[57]Laboratoire de Physique Nucléaire et de Hautes Energies, IN2P3/CNRS, Université Pierre et Marie Curie-Paris6, Université Denis Diderot-Paris7, F-75252 Paris, France
[58]University of Pennsylvania, Philadelphia, Pennsylvania 19104, USA
[59]Università di Perugia, Dipartimento di Fisica and INFN, I-06100 Perugia, Italy
[60]Università di Pisa, Dipartimento di Fisica, Scuola Normale Superiore and INFN, I-56127 Pisa, Italy
[61]Princeton University, Princeton, New Jersey 08544, USA
[62]Università di Roma La Sapienza, Dipartimento di Fisica and INFN, I-00185 Roma, Italy
[63]Universität Rostock, D-18051 Rostock, Germany
[64]Rutherford Appleton Laboratory, Chilton, Didcot, Oxon, OX11 0QX, United Kingdom
[65]DSM/Dapnia, CEA/Saclay, F-91191 Gif-sur-Yvette, France
[66]University of South Carolina, Columbia, South Carolina 29208, USA
[67]Stanford Linear Accelerator Center, Stanford, California 94309, USA
[68]Stanford University, Stanford, California 94305-4060, USA
[69]State University of New York, Albany, New York 12222, USA
[70]University of Tennessee, Knoxville, Tennessee 37996, USA
[71]University of Texas at Austin, Austin, Texas 78712, USA
[72]University of Texas at Dallas, Richardson, Texas 75083, USA
[73]Università di Torino, Dipartimento di Fisica Sperimentale and INFN, I-10125 Torino, Italy
[74]Università di Trieste, Dipartimento di Fisica and INFN, I-34127 Trieste, Italy
[75]IFIC, Universitat de Valencia-CSIC, E-46071 Valencia, Spain
[76]University of Victoria, Victoria, British Columbia, Canada V8W 3P6
[77]Department of Physics, University of Warwick, Coventry CV4 7AL, United Kingdom
[78]University of Wisconsin, Madison, Wisconsin 53706, USA
[79]Yale University, New Haven, Connecticut 06511, USA

(Received 23 December 2007; published 25 April 2008)

We present for the first time a measurement of the weak phase $2\beta + \gamma$ obtained from a time-dependent Dalitz plot analysis of $B^0 \to D^{\mp} K^0 \pi^{\pm}$ decays. Using a sample of approximately 347×10^6 $B\bar{B}$ pairs

[*]Deceased.
[†]Now at Temple University, Philadelphia, PA 19122, USA.
[‡]Now at Tel Aviv University, Tel Aviv, 69978, Israel.
[§]Also with Università di Perugia, Dipartimento di Fisica, Perugia, Italy.
[‖]Also with Università della Basilicata, Potenza, Italy.
[¶]Also with Università di Sassari, Sassari, Italy.

collected by the *BABAR* detector at the PEP-II asymmetric-energy storage rings and assuming the ratio r of the $b \to u$ and $b \to c$ decay amplitudes to be 0.3, we obtain $2\beta + \gamma = (83 \pm 53 \pm 20)^\circ$ and the equivalent solution at $+180^\circ$. The magnitudes and phases for the resonances associated with the $b \to c$ transitions are also extracted from the fit.

DOI: 10.1103/PhysRevD.77.071102 PACS numbers: 12.15.Hh, 11.30.Er, 13.25.Hw, 14.40.Nd

The weak phase $\gamma \equiv \arg(-\frac{V_{ud}V_{ub}^*}{V_{cd}V_{cb}^*})$, where V_{ij} are elements of the Cabibbo-Kobayashi-Maskawa quark-mixing matrix [1], is the least constrained angle of the unitarity triangle [2]. Over the past few years, several methods [3] have been employed to measure γ directly in charged $B \to D^{(*)}K^{(*)}$ decays [4], where sensitivity to the weak phase arises from interference between the $b \to c$ (favored) and $b \to u$ (suppressed) transitions. In addition, decays to two-body final states containing charm have been studied, such as $B^0 \to D^{(*)\mp}\pi^\pm$ and $B^0 \to D^\mp\rho^\pm$ [5] which are sensitive to the weak phase $2\beta + \gamma$ due to B^0-$\bar{B}^0$ mixing. The phase $\beta \equiv \arg(-\frac{V_{cd}V_{cb}^*}{V_{td}V_{tb}^*})$ is well measured in neutral B decays to charmonium final states [6]. The sensitivity of this method is limited by the ratio r between the $b \to u$ and $b \to c$ transitions, which is expected to be very small (~ 0.02). Three-body B decays have been suggested [7] as a way to avoid this limitation, since r in these decays could be as large as 0.4 in some regions of the Dalitz plot.

In this paper we report on the first measurement of the weak phase $2\beta + \gamma$ obtained from a time-dependent Dalitz plot analysis of the decay $B^0 \to D^\mp K^0\pi^\pm$ [8] (charge conjugation is implied throughout the paper). In the decay $B^0 \to D^\mp K^0\pi^\pm$ the three-body final state is reached predominantly through intermediate $B^0 \to \overset{(-)}{\mathrm{D}}{}^{**0}K_S^0$ and $B^0 \to D^-K^{*+}$ decays. In the first case, $\overset{(-)}{\mathrm{D}}{}^{**0}$ indicates a $D_0^*(2400)$ or a $D_2^*(2460)$ state produced through $b \to u$ and $b \to c$ color-suppressed transitions. In the second case, $K^*(892)$, $K_0^*(1430)$, $K_2^*(1430)$, and $K^*(1680)$ are produced through $b \to c$ tree-level transitions. A small contribution from the $b \to u$ decay $B^0 \to D_s^{*+}(2573)\pi^-$ is also expected.

Defining $\vec{x}$ as the vector of the two invariant masses squared $m^2(K_S^0\pi^\pm)$ and $m^2(D^\pm\pi^\mp)$, the amplitude A at each point $\vec{x}$ of the Dalitz plot can be parameterized as a coherent sum of two-body decay matrix elements according to the isobar model [9]:

$$A_{c(u)}(\vec{x})e^{i\phi_{c(u)}(\vec{x})} = \sum_j a_j e^{i\delta_j} BW(\vec{x}; M_j, \Gamma_j, s_j), \quad (1)$$

where c (u) indicates the $b \to c$ ($b \to u$) transition and ϕ is the total strong phase. Each resonance j is parameterized by a magnitude a_j, a phase δ_j, and a factor $BW(\vec{x}; M_j, \Gamma_j, s_j)$ giving the Lorentz invariant expression for the matrix element of the resonance as a function of the position $\vec{x}$, the spin s, the mass M, and the decay width Γ.

The time-dependent probability of a B^0 or $\bar{B}^0$ initial state to decay to a final state with a D^+ or D^- can be expressed as [7]

$$\begin{aligned} P(\vec{x}, \Delta t, \xi, \eta) = \frac{A_c(\vec{x})^2 + A_u(\vec{x})^2}{2} \times \frac{e^{-(|\Delta t|/\tau_B)}}{4\tau_B} \\ \times \{1 - \eta\xi C(\vec{x}) \cos(\Delta m_d \Delta t) \\ + \xi S_\eta(\vec{x}) \sin(\Delta m_d \Delta t)\}. \end{aligned} \quad (2)$$

Here:

$$\begin{aligned} S_\eta(\vec{x}) &= \frac{2\,\mathrm{Im}(A_c(\vec{x})A_u(\vec{x})e^{i(2\beta+\gamma)+\eta i(\phi_c(\vec{x})-\phi_u(\vec{x}))})}{A_c(\vec{x})^2 + A_u(\vec{x})^2}, \\ C(\vec{x}) &= \frac{A_c(\vec{x})^2 - A_u(\vec{x})^2}{A_c(\vec{x})^2 + A_u(\vec{x})^2}, \end{aligned} \quad (3)$$

where Δt is the difference in proper decay times of the reconstructed meson B_{rec} and the flavor-tagging meson B_{tag}, $\xi = +1(-1)$ if the flavor of the B_{rec} is a $B^0(\bar{B}^0)$, and $\eta = +1(-1)$ if the final state contains a $D^+(D^-)$. We use the world averages for the B^0 lifetime τ_B and the mass-eigenstate difference Δm_d [10].

Because Eq. (2) contains the terms $BW^j(\vec{x}, m, \Gamma, s)$, which vary over the Dalitz plot, we can fit the magnitudes a_j and the phases δ_j of Eq. (1) to determine $2\beta + \gamma$ with only a twofold ambiguity [7]. Most of the sensitivity to $2\beta + \gamma$ is expected to come from the interference between $b \to u$ and $b \to c$ transitions leading to $D^{**0}K_S^0$ final states (with expected $r \sim 0.4$), and from the interference of the former with the $b \to c$ transition of the decay $B^0 \to D^-K^{*+}$.

The analysis is based on 347×10^6 $B\bar{B}$ pairs collected at the $\Upsilon(4S)$ resonance by the *BABAR* detector at the PEP-II storage rings. The detector is described in detail elsewhere [11]. In order to estimate signal selection efficiencies and to study physics backgrounds, a Monte Carlo simulation based on GEANT4 [12] is used.

We reconstruct D^+ mesons in the decay mode $K^-\pi^+\pi^+$. The tracks from D^+ decay are required to originate from a common vertex, and the kaon is selected using a likelihood based particle identification algorithm. The D^+ candidates are required to have a mass within ± 12 MeV/c^2 (2σ) of the nominal D^+ mass [10], where σ is the experimental resolution. Oppositely charged tracks from a common vertex are recognized as K_S^0 candidates if they have an invariant mass within ± 7 MeV/c^2 (3σ) of the nominal K_S^0 mass [10] and a transverse flight-length significance 4σ greater than zero. The π^- candidate is a track for which the particle identification is inconsistent with its being a kaon or an electron.

To form B^0 candidates, each D^+ candidate is combined with a K^0_S candidate and a π^- candidate requiring that the three particles originate from a common vertex. We reject B^0 candidates with $m^2(K^0_S\pi^\pm)$ in the window [3.40, 3.95] GeV$^2/c^4$ in order to remove backgrounds with nonzero CP content arising from $B^0 \to D^\mp D^\pm_{(s)}$ decays. Using the beam energy in the e^+e^- center-of-mass (CM) frame, two kinematic variables are constructed: the beam-energy substituted mass $m_{ES} \equiv \sqrt{s/4 - p^{*2}_B}$, and the difference between the measured B^0 candidate energy and the beam energy, $\Delta E \equiv E^*_B - \sqrt{s}/2$. Here p^*_B and E^*_B are the momentum and the energy of the B_{rec} in the CM frame, respectively. Candidates with ΔE in the range $[-0.1, 0.1]$ GeV and m_{ES} in the range $[5.24, 5.29]$ GeV$/c^2$ are selected. We require $|\cos\theta_B|$, the absolute value of the cosine of the angle between the B_{rec} momentum and the beam axis, be less than 0.85, and $|\cos\theta_T|$, the absolute value of the cosine of the angle between the thrust axis of the B_{rec} decay products and the thrust axis of the rest of the event (ROE), be less than 0.95, both in the CM frame [13].

The difference of proper-time Δt of the two Bs in the event is calculated from the measured separation Δz between the vertices of the B_{rec} and the B_{tag} along the beam direction [6]. We accept events with calculated Δt uncertainty less than 2.5 ps and $|\Delta t| < 20$ ps. The average Δt resolution is approximately 1.1 ps. The flavor of the B_{tag} is identified from particles that do not belong to the B_{rec} using a multivariate algorithm [6]. The effective efficiency of the tagging algorithm, defined as $Q = \Sigma_k \epsilon_k (1 - 2w_k)^2$, is $(30.1 \pm 0.5)\%$, where ϵ_k and w_k are the efficiency and the mistag probability, respectively, for each of the six tagging categories k. A separate seventh category contains the untagged events, about 38% of the sample, which contribute to the determination of magnitudes and phases of the resonances and correspond to the case $\xi = 0$ in Eq. (2).

To further suppress the dominant continuum background, which has a more jetlike shape than $B\bar{B}$ events, we use a linear combination $\mathcal{F}$ of five variables: $L_0 = \sum_i p_i$, $L_2 = \sum_i p_i |\cos\theta_i|^2$, the global thrust of the event, $|\cos\theta_T|$, and $|\cos\theta_B|$. Here, p_i is the momentum and θ_i is the angle, with respect to the thrust axis of the B_{rec}, of the tracks and clusters of the ROE in the CM frame. The coefficients of $\mathcal{F}$ are chosen to maximize the separation between the distributions obtained from Monte Carlo simulated signal events and 28 fb^{-1} of continuum events collected at a CM energy 40 MeV below that of the $\Upsilon(4S)$ resonance (off resonance), whose energy is rescaled to the energy of the beams. The correlations among the set of measured values of the variables (m_{ES}, ΔE, $\mathcal{F}$) are negligible. Since both $\mathcal{F}$ and the flavor tagging utilize the ROE information, the distribution of $\mathcal{F}$ is correlated with the tagging category. To take into account this correlation, we parameterize the $\mathcal{F}$ distribution for each tagging category separately.

Approximately 7% of selected events contain more than one reconstructed signal candidate, arising primarily from multiple D^+ candidates. We select the one having the D-candidate mass nearest to the nominal value [10]. For simulated signal events, the entire selection chain has an efficiency of $(9.9 \pm 0.1)\%$, where the error is statistical only.

To separate signal from background and to determine their yields, we first perform an unbinned extended maximum likelihood fit to the selected on-resonance data sample in the variables m_{ES}, ΔE, and $\mathcal{F}$. The role of this first step fit is to extract all the shape parameters, the fractions of events by tagging category, and the overall yields, which will then be fixed in the subsequent time-dependent fit to the Dalitz plot. We define the logarithm of the likelihood:

$$\ln \mathcal{Y} = \sum_{k=1}^{7} \left(\sum_{i=1}^{N_{tot}} \ln \left(\sum_j N_{jk} Y^i_{jk} \right) - \sum_j N_{jk} \right), \qquad (4)$$

where Y^i_{jk} is the product of the probability density functions (PDFs) of m_{ES}, ΔE, and $\mathcal{F}_k$ for the event i in the tagging category k. N_{tot} is the total number of events and N_{jk} is the number of events of each sample component j: signal (Sig), continuum (Cont), combinatoric $B\bar{B}$ decays ($b\bar{b}$), and $B\bar{B}$ events that peak in m_{ES} but not in the ΔE signal region (Peak).

The signal is described by a Gaussian function for the m_{ES} distribution, two Gaussian functions with common mean for the ΔE distribution, and a Gaussian function with different widths on each side of the mean ("bifurcated Gaussian function") for the $\mathcal{F}$ distribution. The signal model parameters are obtained from a fit to a high-statistics data control sample of $B^0 \to D^\mp a^\pm_1$ decays. The selection of these events is similar to that of the signal, except that no K^0_S candidate is required. The decay chain $a^\pm_1 \to \rho^0\pi^\pm$ with $\rho^0 \to \pi^\pm\pi^\mp$ is reconstructed requiring the dipion invariant mass be within ± 150 MeV$/c^2$ of the nominal ρ^0 mass [10], and the invariant mass of the ρ candidate with the third pion be within ± 250 MeV$/c^2$ of the nominal $a^\pm_1$ mass [10].

The m_{ES} distributions of the continuum and combinatoric $B\bar{B}$ backgrounds are described by empirical threshold functions [14], while for ΔE distributions linear functions are used. The $\mathcal{F}$ distributions are parameterized by a bifurcated Gaussian function for the continuum background and a sum of two Gaussian functions for the $B\bar{B}$ combinatoric background. For the latter the parameters are determined by $B\bar{B}$ Monte Carlo simulation. All the shape parameters of the continuum background are taken from fitting the off-resonance data.

The m_{ES} distribution of the Peak background is parameterized by a Gaussian function with the same mean as the signal and a width fixed to the value obtained from Monte Carlo simulation. The ΔE distribution is described

by an exponential function. The $\mathcal{F}$ distribution of Peak is described using the same PDF as for $B\bar{B}$ background.

The yields and the fraction of events for each tagging category are fitted together with the free shape parameters. The yields obtained for each component are $N_{\rm Sig} = 558 \pm 34$, $N_{\rm Cont} = 13\,222 \pm 226$, $N_{b\bar{b}} = 5647 \pm 213$, and $N_{\rm Peak} = 183 \pm 41$, in agreement with the previous result [15].

The second stage of the analysis is the time-dependent fit to the Dalitz plot. For each background component, the Δt distribution is modeled as an exponential, with an effective lifetime parameter. To model the detector resolution, it is convolved with the sum of three Gaussians, the sum of two Gaussians, and one Gaussian in the case of continuum background, $B\bar{B}$ combinatorial background, and Peak, respectively. The widths of the Gaussians, the relative fraction of them, the effective dilution parameters, and the effective lifetimes are determined independently from fits to the control samples: the off-resonance data sample for the continuum background, the $B\bar{B}$ Monte Carlo sample for $B\bar{B}$ combinatorial background and the Peak component. In the case of Peak the lifetime is fixed to the B^0 lifetime [10]. The Δt parameterizations described above for each background component are combined in a global time-dependent PDF, $\mathcal{T}^i_{\pm,\rm Bkgd}$, obtained as a weighted average based on the fitted yields, where $+$ ($-$) indicates $B_{\rm tag} = B^0$ ($B_{\rm tag} = \bar{B}^0$).

To obtain the PDF describing the Dalitz plot of the background in the tagging category k, we use the results of the yields fit and calculate for each event a background weight [16]:

$$W^k_{\rm Bkgd} = 1 - W^k_{\rm Sig} \equiv 1 - \frac{\sum_j \mathbf{V}_{{\rm Sig},j} Y_{jk}(m_{ES}, \Delta E \mathcal{F}_k)}{\sum_j N_j Y_{jk}(m_{ES}, \Delta E, \mathcal{F}_k)}, \quad (5)$$

where N_j is the number of events in a given sample component j [see Eq. (4)], Y_{jk} is defined as in Eq. (4), and $\mathbf{V}_{{\rm Sig},j}$ is the signal row of the covariance matrix of the component yields obtained from the likelihood fit. In the absence of correlations, $W_{\rm Bkgd}$ are the background probabilities $P_{\rm Bkgd}/P_{\rm total}$. Applying these weights to the Dalitz plot of on-resonance data we obtain the observed background Dalitz plot PDF, $\mathcal{D}_{\rm Bkgd}$.

For the signal the effect of finite Δt resolution is described by convolving Eq. (2) with a resolution function composed of three Gaussian distributions. Incorrect tagging dilutes the coefficient of $\cos(\Delta m_d \Delta t)$ in Eq. (2) by a factor $(1 - 2w_i)$. The parameters of the resolution function and those associated with flavor tagging are fixed to the values obtained in [6].

The expression for the time-dependent Dalitz plot likelihood function is then

$$\ln\mathcal{L} = \sum_{k=1}^{7}\Big[\sum_{B^0{\rm tag}} \ln\mathcal{L}_{+,k} + \sum_{\bar{B}^0{\rm tag}} \ln\mathcal{L}_{-,k}\Big], \quad (6)$$

The likelihood function $\mathcal{L}_{+,k}$ ($\mathcal{L}_{-,k}$) for an event in the tagging category k with $B_{\rm tag} = B^0$ ($B_{\rm tag} = \bar{B}^0$) is

$$\mathcal{L}_{\pm,k} = N^k_{\rm Sig}\mathcal{P}^k_{\pm,\rm Sig}Y^k_{\rm Sig} + N^k_{\rm Bkgd}\mathcal{D}_{\rm Bkgd}\mathcal{T}'^k_{\pm,\rm Bkgd}Y^k_{\rm Bkgd}. \quad (7)$$

Here Y indicates the product of PDFs for $m_{\rm ES}$, ΔE, and $\mathcal{F}_k$; $\mathcal{P}_{\pm,\rm Sig}$ is the time-dependent Dalitz plot PDF for signal. The $Y_{\rm Bkgd}$ parameterization is obtained from a weighted average, using the fitted yields, of the shapes obtained from the first step fit.

With the current data set we are unable to determine the magnitudes for the suppressed $b \to u$ decays. We therefore fix the ratio $r = \frac{A(b\to u)}{A(b\to c)} = 0.3$ for each resonance in the PDF, which is compatible with the limit $r < 0.4$ (90% C.L.) reported in Ref. [17]. The $D_s^{*+}(2573)$ magnitude and phase are fixed to the values given in [8]. Despite the fact that the $b \to u$ phases cannot be precisely determined, they are left free in the fit. All the $b \to c$ magnitudes and phases together with $2\beta + \gamma$ are free parameters. The whole fitting procedure has been validated using high statistic parameterized (toy) Monte Carlo samples.

The fit is performed on events satisfying $m_{\rm ES} > 5.27$ GeV/c^2, $|\Delta{\rm E}| < 50$ MeV, and $\mathcal{F} > -2$. Results are shown in Table I. Figure 1 shows the projections of the on-resonance data sample on the two Dalitz plot variables $m^2(K^0_S\pi^\pm)$ and $m^2(D^\pm\pi^\mp)$ with the fitted PDFs superimposed. Figure 2(a) shows the $m_{\rm ES}$ distribution and the

TABLE I. Results for $2\beta + \gamma$ and the $b \to c$ transitions magnitudes a_c and phases δ_c assuming $r = 0.3$. The first uncertainty is statistical; the second is systematic.

Resonance	Bias correction for the magnitude	a_c magnitude after bias correction	Phase δ_c (°)
$K^*(892)$	···	1	0
$D^*_0(2400)$	+0.003	$0.290 \pm 0.048 \pm 0.067$	$267 \pm 22 \pm 35$
$D^*_2(2460)$	−0.033	$0.042 \pm 0.050 \pm 0.048$	$325 \pm 46 \pm 20$
$K^*_0(1430)$	−0.025	$0.135 \pm 0.058 \pm 0.099$	$284 \pm 30 \pm 11$
$K^*_2(1430)$	−0.017	$0.108 \pm 0.056 \pm 0.051$	$221 \pm 30 \pm 14$
$K^*(1680)$	−0.011	$0.404 \pm 0.047 \pm 0.046$	$128 \pm 22 \pm 24$
$2\beta + \gamma = (83 \pm 53 \pm 20)°$ and $(263 \pm 53 \pm 20)°$			

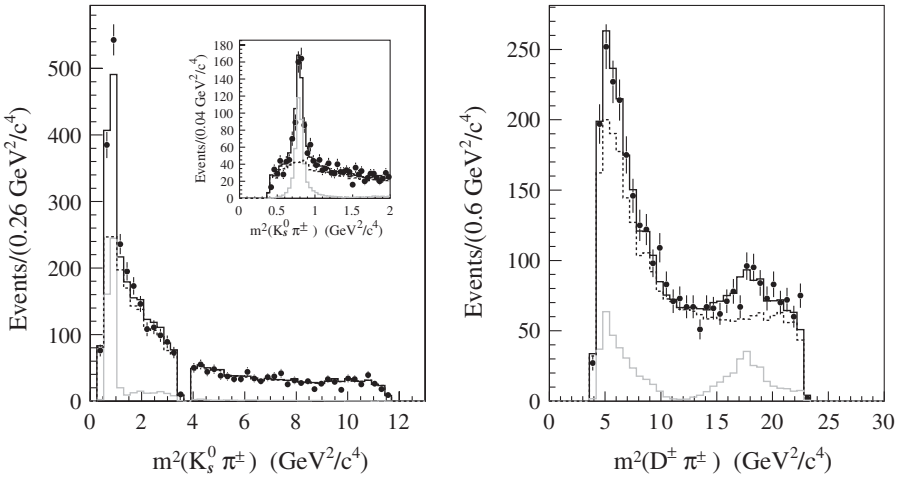

FIG. 1. The distributions of $m^2(K^0_S\pi)$ and $m^2(D\pi)$ in data (solid points). The overall PDF is superimposed (black line). The gray full line is the signal PDF; the dashed black line is the background PDF.

fitted PDFs for each component, after applying additional requirements on ΔE and $\mathcal{F}$. Besides the value of $2\beta + \gamma$, an important outcome of the analysis is the fit of the resonance contributions to the $b \to c$ part of the Dalitz plot. Biases related to the small sample size are observed in the measurement of the magnitudes. They are estimated using a large number of toy Monte Carlo experiments generated with the magnitudes values obtained in the fit to the on-resonance data sample.

The systematic errors are summarized in Table II. The main contribution is related to the parameterization of the background Dalitz plot. This effect has been estimated by repeating the fit with a parameterization obtained from off-resonance data and $B\bar{B}$ generic Monte Carlo simulation. The systematic uncertainty due to the efficiency variation over the Dalitz plot has been evaluated assuming a flat efficiency. The effect of potential CP content of the $B\bar{B}$ peaking background is taken into account assuming the same CP violation structure as in the signal with a value $r_{\rm eff} = 0.4$. The systematic uncertainties on the signal Dalitz plot come from the variation of the r factor (0.3 ± 0.1) and of the $D_s^{*+}(2573)$ magnitude (0.02 ± 0.01) and from the introduction of up to 7% of a nonresonant component. In addition, the masses and widths of the resonances have been varied by 1 standard deviation [10]. We obtain the systematic uncertainty arising from imperfect knowledge of the $\mathcal{Y}$ shape parameters and the yields by varying all fixed parameters within their uncertainties. Similar variations are applied to the signal and background fractions in each tagging category as well as for the Δt

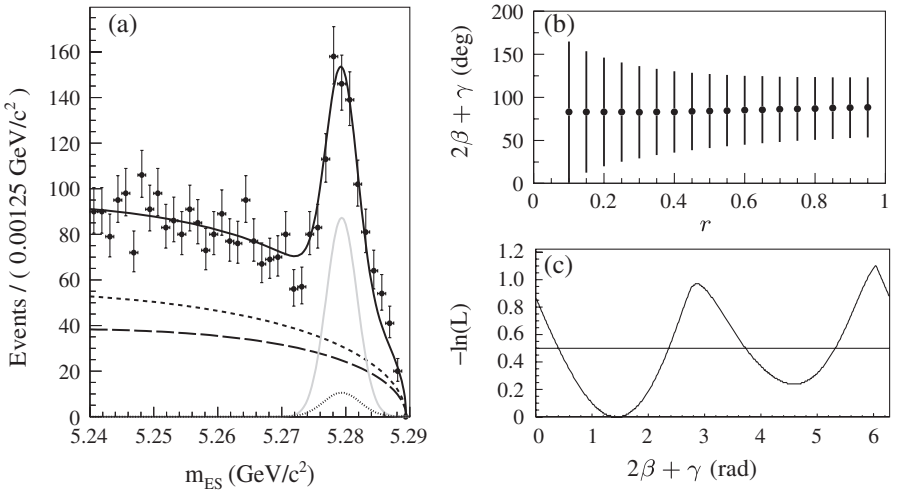

FIG. 2. (a) The $m_{\rm ES}$ distribution of on-resonance data (solid points) for the global fitted PDF (black line) with the contribution of the PDF for each component superimposed: signal (gray line), continuum (small dashed line), combinatoric $B\bar{B}$ (large dashed line), and Peak (dotted line). To enhance the signal $|\Delta E| < 0.025$ GeV and $\mathcal{F} > 0.2$ have been required. (b) Distribution of the values of $2\beta + \gamma$ fitted on data for different hypotheses on the r value. (c) Variation of the logarithm of the likelihood with $2\beta + \gamma$.

TABLE II. Sources and sizes of systematic errors.

Systematic	$2\beta+\gamma$	$D_0^*(2400)$		$D_2^*(2460)$		$K_0^*(1430)$		$K_2^*(1430)$		$K^*(1680)$	
		a_c	δ_c	a_c	δ_c	a_c	δ_c	a_c	δ_c	a_c	δ_c
Background Dalitz plot param.	16.0°	0.058	3.2°	0.034	12.1°	0.088	9.5°	0.005	12.0°	0.015	10.3°
Efficiency over the Dalitz plot	5.8°	0.014	17.5°	0.028	10.8°	0.005	1.9°	0.036	0.8°	0.017	19.4°
CP content of bkgd.	1.0°	0.021	6.9°	0.003	8.4°	0.005	1.4°	0.007	3.9°	0.003	1.0°
r	1.0°	0.013	8.6°	0.013	2.2°	0.039	3.0°	0.012	0.7°	0.016	0.3°
$a(D_s^{*+}(2573))$	0.7°	...	...	...	...	...	...	...	...	...	...
m, Γ	9.5°	0.012	28.0°	0.011	6.9°	0.018	2.8°	0.032	5.9°	0.036	9.3°
$\mathcal{Y}$ PDF param.	3.0°	0.005	1.4°	0.002	0.4°	0.007	0.6°	0.003	0.1°	0.002	0.5°
Signal and bkgd. frac.	1.4°	0.012	2.9°	0.004	1.2°	0.013	1.4°	0.008	0.7°	0.004	1.4°
Yields	0.1°	0.003	1.3°	0.001	0.3°	0.005	0.4°	0.002	0.1°	0.002	0.1°
Tagging and time param.	2.6°	0.003	1.4°	0.001	0.3°	0.004	0.4°	0.002	0.2°	0.002	0.2°

resolution parameters, the effective lifetimes, the B lifetime τ_B, and the mixing frequency Δm_d. The systematic uncertainties due to the dependence of the tagging efficiency on the B flavor, the beam spot position, and the SVT alignment have been obtained following the procedure described in [6].

Figure 2(b) shows the dependence of the measurement of $2\beta+\gamma$ on r. For each fixed value of r, a point in the plot represents the result of the fit on $2\beta+\gamma$ with its statistical error. The error decreases, as expected, for increasing r, and the central value remains stable. The projection on $2\beta+\gamma$ of the negative logarithm of the likelihood in Fig. 2(c) clearly shows the minimum corresponding to the result of the fit and the expected mirror solution at $+\pi$ rad. Having fixed some magnitudes and strong phases, the second solution is disfavored, but it should be regarded as equivalent.

In summary, we present the first results of a time-dependent Dalitz plot analysis of the decay $B^0 \to D^{\pm}K^0\pi^{\mp}$ to determine the Dalitz plot model parameters and the weak phase $2\beta+\gamma$. Assuming $r=0.3$ we find $2\beta+\gamma=(83\pm53\pm20)°$ and the equivalent solution at $+180°$, where the first error is statistical and the second is systematic.

We are grateful for the extraordinary contributions of our PEP-II colleagues in achieving the excellent luminosity and machine conditions that have made this work possible. The success of this project also relies critically on the expertise and dedication of the computing organizations that support *BABAR*. The collaborating institutions wish to thank SLAC for its support and the kind hospitality extended to them. This work is supported by the Department of Energy and National Science Foundation (USA), the Natural Sciences and Engineering Research Council (Canada), the Commissariat à l'Energie Atomique and Institut National de Physique Nucléaire et de Physique des Particules (France), the Bundesministerium für Bildung und Forschung and Deutsche Forschungsgemeinschaft (Germany), the Istituto Nazionale di Fisica Nucleare (Italy), the Foundation for Fundamental Research on Matter (The Netherlands), the Research Council of Norway, the Ministry of Science and Technology of the Russian Federation, Ministerio de Educación y Ciencia (Spain), and the Science and Technology Facilities Council (United Kingdom). Individuals have received support from the Marie-Curie IEF program (European Union) and the A. P. Sloan Foundation.

[1] N. Cabibbo, Phys. Rev. Lett. **10**, 531 (1963); M. Kobayashi and T. Maskawa, Prog. Theor. Phys. **49**, 652 (1973).

[2] M. Bona *et al.* (UTfit Collaboration), J. High Energy Phys. 10 (2006) 081; J. Charles *et al.* (CKMfitter Group), Eur. Phys. J. C **41**, 1 (2005); M Pivk, in *High Energy Physics, ICHEP 2004: Proceedings of the 32nd International Conference, Beijing, China, 16–22 August 2004*, edited by H. Chen, D. Du, W. Li, and C. Luvol (World Scientific, Singapore, 2005), Vol. 2, p. 909.

[3] M. Gronau and D. London, Phys. Lett. B **253**, 483 (1991); M. Gronau and D. Wyler, Phys. Lett. B **265**, 172 (1991); I. Dunietz, Phys. Lett. B **270**, 75 (1991); Z. Phys. C **56**, 129 (1992); D. Atwood, G. Eilam, M. Gronau, and A. Soni, Phys. Lett. B **341**, 372 (1995); D. Atwood, I. Dunietz, and A. Soni, Phys. Rev. Lett. **78**, 3257 (1997); A. Giri, Yu. Grossman, A. Soffer, and J. Zupan, Phys. Rev. D **68**, 054018 (2003).

[4] B. Aubert *et al.* (*BABAR* Collaboration), Phys. Rev. Lett. **95**, 121802 (2005); A. Poluetkov *et al.* (Belle Collaboration), Phys. Rev. D **73**, 112009 (2006); B. Aubert *et al.* (*BABAR* Collaboration), Phys. Rev. D **73**, 051105 (2006); K. Abe *et al.* (Belle Collaboration), Phys. Rev. D **73**, 051106 (2006); B. Aubert *et al.* (*BABAR*

Collaboration), Phys. Rev. D **71**, 031102 (2005); **72**, 071103 (2005); arXiv:0708:0182; Phys. Rev. D **72**, 032004 (2005); M. Saigo *et al.* (Belle Collaboration), Phys. Rev. Lett. **94**, 091601 (2005); B. Aubert *et al.* (*BABAR* Collaboration), Phys. Rev. D **72**, 071104 (2005).

[5] B. Aubert *et al.* (*BABAR* Collaboration), Phys. Rev. D **73**, 111101 (2006); Phys. Rev. D **71**, 112003 (2005).

[6] B. Aubert *et al.* (*BABAR* Collaboration), Phys. Rev. Lett. **94**, 161803 (2005).

[7] M. Gronau, Phys. Lett. B **557**, 198 (2003); R. Aleksan, T. C. Petersen, and A. Soffer, Phys. Rev. D **67**, 096002 (2003); R. Aleksan and T. C. Petersen, in *Proceedings of the CKM03 Workshop, Durham, 2003*, econf C 0304052, WG414 (2003).

[8] F. Polci, M.-H. Schune, and A. Stocchi, arXiv.org:hep-ph/0605129.

[9] S. Kopp *et al.* (CLEO Collaboration), Phys. Rev. D **63**, 092001 (2001); H. Muramatsu *et al.* (CLEO Collaboration), Phys. Rev. Lett. **89**, 251802 (2002); **90**, 059901(E) (2003).

[10] W.-M. Yao *et al.* (Particle Data Group), J. Phys. G **33**, 1 (2006).

[11] B. Aubert *et al.* (*BABAR* Collaboration), Nucl. Instrum. Methods Phys. Res., Sect. A **479**, 1 (2002).

[12] S. Agostinelli *et al.* (GEANT4 Collaboration), Nucl. Instrum. Methods Phys. Res., Sect. A **506**, 250 (2003).

[13] E. Farhi, Phys. Rev. Lett. **39**, 1587 (1977).

[14] H. Albrecht *et al.* (ARGUS Collaboration), Phys. Lett. B **185**, 218 (1987); **241**, 278 (1990).

[15] B. Aubert *et al.* (*BABAR* Collaboration), Phys. Rev. Lett. **95**, 171802 (2005).

[16] M. Pivk and F. R. Le Diberder, Nucl. Instrum. Methods Phys. Res., Sect. A **555**, 356 (2005).

[17] B. Aubert *et al.* (*BABAR* Collaboration), Phys. Rev. D **74**, 031101 (2006).